

## Projectile Fragmentation of the Extremely Neutron-Rich Nucleus $^{11}\text{Li}$ at 0.79 GeV/nucleon

T. Kobayashi and O. Yamakawa

*National Laboratory for High Energy Physics (KEK), Tsukuba, Ibaraki, 305 Japan*

K. Omata,

*Institute for Nuclear Study, University of Tokyo, Tanashi, Tokyo, 188 Japan*

K. Sugimoto, T. Shimoda, and N. Takahashi,

*Faculty of Science, Osaka University, Toyonaka, Osaka, 560 Japan*

and

I. Tanihata

*The Institute of Physical and Chemical Research (RIKEN), Wako, Saitama, 351-01 Japan*

(Received 25 September 1987)

Projectile fragmentations of  $^{11}\text{Li}$ ,  $^8\text{He}$ , and  $^6\text{He}$  have been measured at 0.79 GeV/nucleon. Production cross sections and momentum distributions of the produced isotopes ( $Z \geq 2$ ) are measured inclusively. Transverse-momentum distributions of  $^9\text{Li}$  from the fragmentation of  $^{11}\text{Li}$  show two Gaussian components of different widths. The width of the wide component is consistent with the values observed in the fragmentation of stable nuclei, whereas the other component shows an extremely narrow width reflecting the weak binding of the two outer neutrons in the  $^{11}\text{Li}$  nucleus.

PACS numbers: 25.70.Np, 21.10.Gv, 27.20.+n

Projectile fragmentation is one of the most common processes observable in nucleus-nucleus collisions in the energy range of a few gigaelectronvolts per nucleon. The projectile fragmentations of  $^{12}\text{C}$  and  $^{16}\text{O}$  were intensively studied by Greiner *et al.*<sup>1</sup> at 1.0 and 2.1 GeV/nucleon. The fragment momentum distribution shows an isotropic Gaussian distribution in the projectile rest frame. The width of the distribution can be understood in terms of Fermi motion or a temperature corresponding to the nuclear binding energy.<sup>2</sup> Later Fujita and Hüfner<sup>3</sup> analyzed the momentum distribution of the projectile fragment in the one-nucleon-removal channel. It was shown that the momentum distribution of the nucleon in a beam nucleus can be deduced from the observed momentum distribution of the fragment.

A newly developed technique to produce a high-quality  $\beta$ -unstable nuclear beam<sup>4</sup> provides a new possibility to study the nucleon-density distribution and the momentum distribution of nucleons in unstable nuclei through the projectile fragmentation of those exotic nuclei. In this Letter we present the first measurements of fragments produced from the projectile fragmentation of extremely neutron-rich nuclei ( $^{11}\text{Li}$ ,  $^8\text{He}$ , and  $^6\text{He}$ ) at 0.79-GeV/nucleon incident energy, and then show evidence of the existence of a long tail in the neutron distribution of the  $^{11}\text{Li}$  nucleus.

The experiment was carried out at the Bevalac in the Lawrence Berkeley Laboratory. The secondary beams of  $^{11}\text{Li}$ ,  $^8\text{He}$ , and  $^6\text{He}$  were produced through the projectile fragmentation of 0.8-GeV/nucleon  $^{20}\text{Ne}$  or  $^{22}\text{Ne}$  primary beams. The beam line for isotope separation was the

same one as described by Tanihata and co-workers.<sup>4,5</sup> The energy of the secondary beam on the target was  $0.79 \pm 0.02$  GeV/nucleon. A carbon ( $5.2 \text{ g/cm}^2$ ) and a lead ( $6.6 \text{ g/cm}^2$ ) target were used. Projectile fragments ( $Z \geq 2$ ) were measured inclusively at zero degrees with the magnetic spectrometer (HISS) equipped with a scintillation hodoscope, multiwire proportional chambers, and drift chambers. The rigidity acceptance and angular acceptance of the spectrometer were  $\pm 20\%$  and  $\pm 2.0^\circ$ , respectively. The detector system had overall vertical-scattering-angle resolution of 0.9 mrad which is most important for precise transverse-momentum measurement. Contribution of multiple Coulomb scattering in the target to the vertical-scattering-angle resolution is  $3.7q/m$  mrad and  $11.9q/m$  mrad for carbon and lead targets, respectively, where  $q/m$  is charge/mass ratio of the fragment. Charge of beam and fragment was measured by scintillator stacks. Charge resolution  $\sigma_z$  was 0.08 charge unit. Fragments were identified by charge and rigidity measurements. Mass resolution  $\sigma_A$  from the rigidity measurement was 0.09 mass unit. In order to cover a wide rigidity range (2.3 to 6.0 GeV/ $c$ ) of fragments, the magnetic field of the HISS dipole was adjusted for each mass/charge ratio of the fragment.

Transverse-momentum distributions of the fragments perpendicular to the bending plane are analyzed. Although parallel-momentum distributions were not measured accurately in the present experiment because of the rigidity resolution of the detector system and momentum dispersion of the secondary beam itself, the widths of the parallel- and transverse-momentum distri-

butions are known to be equal within  $\pm 10\%$ .<sup>1</sup> The momentum distributions of He isotopes from the fragmentation of  ${}^6\text{He}$  and  ${}^8\text{He}$  on a carbon target show a Gaussian shape as shown in Fig. 1(a). The width  $\sigma$  of the momentum distribution can be parametrized, following Goldhaber,<sup>2</sup> by a single parameter  $\sigma_0$  (reduced width) as  $\sigma^2 = \sigma_0^2 F(B-F)/(B-1)$ , where  $F$  is the mass number of the fragment and  $B$  is the mass number of the projectile. The reduced width  $\sigma_0$  of He isotopes is approximately 60 MeV/c. This value is somewhat smaller than the value ( $\approx 78$  MeV/c) obtained from the fragmentation of  ${}^{12}\text{C}$  at 1 GeV/nucleon.

A striking difference is observed in the momentum distribution of  ${}^9\text{Li}$  from the reaction  ${}^{11}\text{Li} + \text{C}$ . The transverse-momentum distribution of  ${}^9\text{Li}$  shows a two-Gaussian-peak structure as seen in Fig. 1(b). The width of the wide component  $\sigma = 95 \pm 12$  MeV/c gives similar  $\sigma_0$  value ( $\sigma_0 = 71 \pm 9$  MeV/c) to that of  ${}^{12}\text{C}$  fragmentation, whereas the other component shows an extremely narrow width:  $\sigma = 23 \pm 5$  MeV/c ( $\sigma_0 = 17 \pm 4$  MeV/c). Two-component structure is also seen in the parallel-momentum distribution, though the resolution was much worse than that of the transverse direction. It should be noted that the narrow component in the transverse direction is correlated with the narrow component in the parallel direction. A two-component structure is also seen in the momentum distribution of  ${}^8\text{Li}$  from the reaction  ${}^{11}\text{Li} + \text{C}$ . The width  $\sigma$  as well as the reduced width  $\sigma_0$  from the present measurement are summarized in

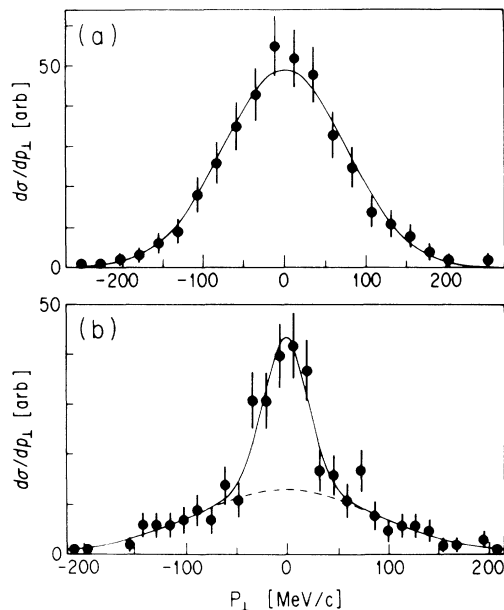


FIG. 1. Transverse-momentum distributions of (a)  ${}^6\text{He}$  fragments from reaction  ${}^8\text{He} + \text{C}$  and (b)  ${}^9\text{Li}$  fragments from reaction  ${}^{11}\text{Li} + \text{C}$ . The solid lines are fitted Gaussian distributions. The dotted line is a contribution of the wide component in the  ${}^9\text{Li}$  distribution.

Table I after correction for detector resolution and multiple Coulomb scattering.

According to Goldhaber's interpretation,  $\sigma_0$  can be related to the Fermi momentum  $P_F$  of the projectile by  $\sigma_0 = P_F/\sqrt{5}$ , if we assume the Fermi-gas model and the sudden approximation. The values of  $\sigma_0$ , except for the narrow component in  ${}^{11}\text{Li}$  fragmentation, are consistent with  $\sigma_0 = 76$  MeV/c reduced from  $P_F = 169$  MeV/c determined from the quasielastic electron scattering from the  ${}^6\text{Li}$  nucleus.<sup>6</sup> On the other hand, if thermal equilibrium is assumed,  $\sigma_0$  can be related to the nuclear temperature  $T$  by  $\sigma_0^2 = M_p T(B-1)/B$ , where  $M_p$  is the nucleon mass. The narrow component gives  $0.34 \pm 0.16$  MeV, whereas the wide component gives  $6.0 \pm 1.5$  MeV. However, it should be noted that these two interpretations stand on completely different physical assumptions. In the interpretation of the Fermi gas, it is difficult to consider two different Fermi momenta in the nucleus. Therefore a simple view based on the Fermi-gas model fails to explain the  ${}^{11}\text{Li}$  fragmentation data. Also it is difficult to understand why two discretely different temperatures appear in the fragment.

In order to understand both the narrow and wide components, we followed the microscopic model of Hüfner and Nemes.<sup>7</sup> According to their analysis, the momentum distribution of one-nucleon-removal fragments reflects the momentum distribution of the removed nucleon at the surface of the projectile. This idea was extended to a several-nucleon-removal channel<sup>8</sup> with the formalism developed by Serber<sup>9</sup> for stripping reactions. Near a nuclear surface, the momentum distribution can be approximated by the Fourier transform of the asymp-

TABLE I. Production cross sections, momentum widths ( $\sigma$ ), and reduced momentum widths ( $\sigma_0$ ) of the projectile fragments measured in the present measurement.

Beam	Target	Fragment	Cross section (mb)	$\sigma$ (MeV/c)	$\sigma_0$ (MeV/c)
${}^{11}\text{Li}$	C	${}^9\text{Li}$	$213 \pm 21$	$95 \pm 12$	$71 \pm 9$
				$23 \pm 5^a$	$17 \pm 4^a$
		${}^8\text{Li}$	$62 \pm 9$	$143 \pm 118$	$92 \pm 76$
				$42 \pm 17^a$	$27 \pm 11^a$
		${}^7\text{Li}$	$33 \pm 8$	...	...
		${}^6\text{Li}$	$7 \pm 3$	...	...
		${}^8\text{He}$	$26 \pm 6$	$99 \pm 19$	$64 \pm 12$
${}^6\text{He}$	C	${}^6\text{He}$	$45 \pm 8$	$81 \pm 12$	$47 \pm 7$
		${}^4\text{He}$	$47 \pm 10$	...	...
		${}^3\text{He}$	$6 \pm 3$	...	...
		${}^9\text{Li}$	$1513 \pm 177$	$71 \pm 15$	$53 \pm 11$
${}^8\text{He}$	C	${}^6\text{He}$	$165 \pm 87$	...	...
		${}^4\text{He}$	$202 \pm 17$	$77 \pm 5$	$59 \pm 4$
${}^6\text{He}$	C	${}^4\text{He}$	$95 \pm 9$	$88 \pm 6$	$58 \pm 4$
		${}^4\text{He}$	$189 \pm 14$	$65 \pm 4$	$51 \pm 3$
		${}^3\text{He}$	$9 \pm 4$	...	...

<sup>a</sup>Momentum width of the narrow component.

otic wave function  $\exp(-kr)/r$ , where  $k$  is expressed as  $k^2 = 2\mu\langle\epsilon\rangle$  with the reduced mass  $\mu$ , and the separation energy  $\langle\epsilon\rangle$ . This starting point is exactly the same as the one used by Friedman.<sup>10</sup> By approximation of the Lorentzian-type momentum-distribution function,  $1/(p^2+k^2)$ , by a Gaussian, it was shown that the width  $\sigma$  of the momentum distribution is expressed as  $\sigma^2 = \sigma_0^2 F(B-F)/(B-1)$ , where  $\sigma_0$  is given as  $\sigma_0^2 = M_p\langle\epsilon\rangle(B-1)/B$ . This expression is identical to that of Goldhaber if the nuclear temperature  $T$  is replaced by the separation energy  $\langle\epsilon\rangle$  of the removed nucleons. The observed narrow width gives  $\langle\epsilon\rangle = 0.34 \pm 0.16$  MeV which can be compared with the separation energy of the two outer neutrons in the  $^{11}\text{Li}$  nucleus;

$$\Delta E(^9\text{Li} + 2n) - (^{11}\text{Li}) = 0.19 \pm 0.11 \text{ MeV},$$

$$\Delta E(^9\text{Li}^* + 2n) - (^{11}\text{Li}) = 2.88 \text{ MeV},$$

and

$$\Delta E(^{10}\text{Li} + n) - (^{11}\text{Li}) = 0.96 \text{ MeV}.$$

The broad width, on the other hand, gives  $\langle\epsilon\rangle = 6.0 \pm 1.5$  MeV which is closer to the normal nucleon separation energy. Therefore it is considered qualitatively that the narrow component is produced by reactions in which the two weakly bound outer neutrons are removed from the  $^{11}\text{Li}$  nucleus. The broader component is due to the following three processes: removal of normally bound neutrons, decay of excited  $^9\text{Li}$ , and decay of particle-unbound  $^{10}\text{Li}$ .

Matter radii of  $^{11}\text{Li}$  and  $^{6,8}\text{He}$  nuclei were determined from the total interaction cross-section measurement at 0.79 GeV/nucleon by Tanihata *et al.*<sup>11</sup> They reported that  $^{11}\text{Li}$  has an extremely large radius ( $3.27 \pm 0.24$  fm) compared with that of  $^9\text{Li}$  ( $2.43 \pm 0.02$  fm) and suggested a large deformation and/or a long tail in the matter distribution of  $^{11}\text{Li}$  nucleus. The present observation of a narrow component in the momentum distribution of  $^9\text{Li}$  from the projectile fragmentation of  $^{11}\text{Li}$  provides additional information on the interpretation of large size. A narrower width ( $k$ ) of the momentum distribution indicates a longer decay constant ( $1/k$ , which is about 8.3 fm in the case of  $^{11}\text{Li}$ ) of the wave function in a space coordinate. Hence the observed narrow momentum distribution indicates the existence of a long neutron tail in the  $^{11}\text{Li}$  nucleus. The present data indicate that the long neutron tail is the cause of the large nuclear-matter radius. This interpretation is also consistent with a recent measurement of the magnetic moment<sup>12</sup> of  $^{11}\text{Li}$ , which suggested that  $^{11}\text{Li}$  is a good spherical nucleus. A more qualitative relation was drawn by Hansen and Jonson<sup>13</sup> between the separation energy of the two outer neutrons and the nuclear-matter radius based on a model in which a dineutron is moving outside the  $^9\text{Li}$  core. Their simple relation agrees quite well with the experimental data. As a result, we can conclude that large matter radius of  $^{11}\text{Li}$

from the interaction cross-section measurement, very small two-neutron separation energy in  $^{11}\text{Li}$  from mass measurement, and narrow momentum distribution of  $^9\text{Li}$  from the fragmentation of  $^{11}\text{Li}$  in the present measurement are consistent with each other and all of them indicate that  $^{11}\text{Li}$  nucleus has a long neutron tail.

Isotope production cross sections for the measured channels are summarized also in Table I after correction for the acceptance and the secondary interaction in the target. Because of the unknown fragmentation cross sections (such as  $^7\text{Li} \rightarrow ^6\text{He} \dots$ ) which are necessary to correct for secondary interactions of the projectile fragments in the target, there is an additional  $\approx 3\%$  ambiguity in the absolute value of the cross sections. Figure 2 shows the Li and He isotope production cross sections from the reaction  $^{11}\text{Li} + \text{C}$ . A naive geometrical consideration of the projectile fragmentation process shows that those partial cross sections are consistent with an existence of a thick neutron skin.<sup>14</sup> However, this naive idea has to be studied carefully because an evaporation process may affect the final cross sections.

In order to understand the fragmentation cross sections in a more quantitative way, a calculation with use of the abrasion-ablation model<sup>15</sup> was made by Harvey.<sup>16</sup> In this model, a cascade-type calculation is used for the abrasion stage to get the excitation energy and the cross section of prefragments. Decay of these prefragments in the ablation (evaporation) stage is calculated by application of  $\exp(-Q/T)$  dependence. The most important assumption in the calculation, which should be verified in the future, is that all the observed He fragments come from the decay of excited Li prefragments because of too high excitation energies of the He prefragments. Without this assumption, it was impossible to explain the tendency of the He production cross sections. A calcula-

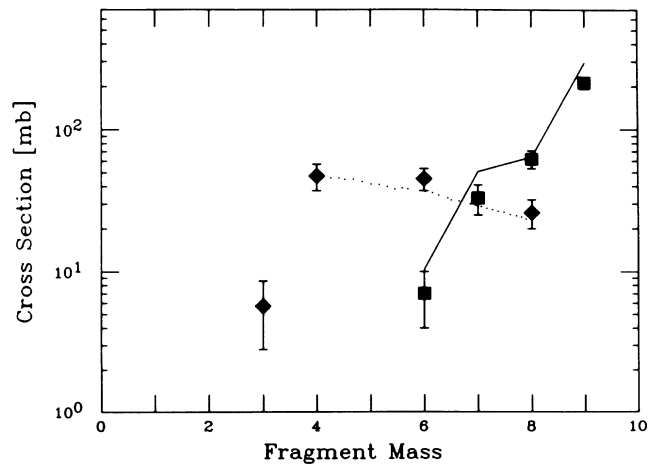


FIG. 2. Production cross sections of He (lozenges) and Li (squares) fragments from the reaction  $^{11}\text{Li} + \text{C}$ . Solid (Li) and dotted (He) lines are from the abrasion-ablation calculation

tion with a Woods-Saxon density distribution was done with  $R_{1/2}(p) = 1.63$  fm,  $R_{1/2}(n) = 2.60$  fm,  $\rho_0(p) = 0.079$  nucleon/fm<sup>3</sup>, and  $\rho_0(n) = 0.085$  nucleon/fm<sup>3</sup>, and the result is also shown in Fig. 2. The agreement of the data and the calculation is consistent with the existence of a thick neutron skin in the <sup>11</sup>Li nucleus. Harvey's calculation also shows that direct production of <sup>9</sup>Li ground state is about 34 mb out of the calculated total <sup>9</sup>Li production cross section of 294 mb, i.e., a large amount of <sup>9</sup>Li is produced from the decay of <sup>10</sup>Li and the excited <sup>9</sup>Li. Fortunately, all these sequential decays are associated with much larger average separation energy  $\langle \epsilon \rangle$  compared with the separation energy of 0.19 MeV which is associated with the direct removal of two neutrons into <sup>9</sup>Li ground state. These backgrounds will only contribute to the wide component. Then it ensures that we can deduce the momentum distribution of the outer two neutrons from the narrow component <sup>9</sup>Li.

Fragmentation channels of <sup>11</sup>Li+Pb→<sup>9</sup>Li and <sup>6</sup>He were also measured. In the collision with a heavy target, contribution from the electromagnetic dissociation process (EMD, i.e., interaction of a projectile with photons from the Coulomb field of a high-Z target) is known to be a dominant process.<sup>17</sup> From the cross-section ratios

$$\sigma(^{11}\text{Li}+\text{Pb} \rightarrow ^9\text{Li})/\sigma(^{11}\text{Li}+\text{C} \rightarrow ^9\text{Li}) = 7.1 \pm 1.1$$

and

$$\sigma(^{11}\text{Li}+\text{Pb} \rightarrow ^6\text{He})/\sigma(^{11}\text{Li}+\text{C} \rightarrow ^6\text{He}) = 3.7 \pm 2.0,$$

it is estimated that the EMD process contributes approximately 50% of the <sup>9</sup>Li production cross section from the lead target, on the assumption that <sup>6</sup>He is produced without the EMD process. The ratio of fragmentation cross section  $\sigma(^{11}\text{Li}+\text{Pb} \rightarrow ^9\text{Li}) = 1513 \pm 177$  mb to the estimated interaction cross section  $\sigma_I(^{11}\text{Li}+\text{Pb}) = 3320$  mb is quite large compared with that for the carbon target;  $\sigma(^{11}\text{Li}+\text{C} \rightarrow ^9\text{Li}) = 213 \pm 21$  mb and  $\sigma_I(^{11}\text{Li}+\text{C}) = 1056 \pm 30$  mb.<sup>11</sup> It suggests that the EMD contribution to the <sup>11</sup>Li+Pb→<sup>9</sup>Li channel is quite large or even that the interaction cross section itself is affected by the EMD process. The recently measured interaction cross section<sup>18</sup>  $\sigma_I(^{11}\text{Li}+\text{Pb}) = 5780 \pm 670$  mb supports the latter interpretation. It has to be noted that the transverse-momentum distribution of the <sup>9</sup>Li fragment shows only a single (and wide) Gaussian component of  $\sigma_0 = 53 \pm 11$  MeV/c. This fact might indicate a smaller fraction of direct neutron(s)-removal contribution which will produce narrow momentum distributions of fragments.

An attempt was also made to search for a <sup>10</sup>He isotope (one proton removal from <sup>11</sup>Li) from the projectile fragmentation of a <sup>11</sup>Li beam on a carbon target. This seems to be a better technique to produce <sup>10</sup>He compared with a spallation method due to kinematic focusing, i.e., 100% detection efficiency, and an expected large one-proton removal cross section. The upper limit of the

<sup>10</sup>He production cross section is 50 μb which should be compared with the nominal one-proton-removal cross section of ≈ 50 mb in the same projectile mass range.

In summary, projectile fragmentations of extremely neutron-rich nuclei, <sup>11</sup>Li, <sup>8</sup>He, and <sup>6</sup>He, were studied for the first time at 0.79-GeV/nucleon incident energy. (1) Momentum distributions of Li fragments from the fragmentation of <sup>11</sup>Li show two components. The narrow width was understood to be originating from the removal of the two weakly bound outer neutrons in the <sup>11</sup>Li nucleus. (2) Isotope production cross sections were measured and analyzed with the abrasion-ablation model. (3) Several observations in the <sup>11</sup>Li nucleus, (i) large root mean square radius, (ii) small momentum fluctuations in the projectile fragmentation, and (iii) small separation energy of the two outer neutrons, suggest the existence of a large neutron halo around the <sup>11</sup>Li nucleus. (4) Momentum distributions and isotope production cross sections from a heavy target suggest that the electromagnetic dissociation process is also important in the fragmentation of neutron-rich nuclei from a heavy target.

We express our sincere thanks to all the members of the HISS group and the Bevalac staff for their excellent support during the run. Thanks also go to Dr. B. G. Harvey for performance of the calculation of the abrasion-ablation model, and to Mr. Y. Matsuyama for his technical assistance. This work was supported by the Director, Division of Nuclear Physics of the Office of High-Energy and Nuclear Physics of the U.S. Department of Energy under Contract No. DE-AC03-76SF00098, by the Institute for Nuclear Study-Lawrence Berkeley Laboratory Collaboration Program, and by the Japan-U.S. Joint Program for High-Energy Physics.

<sup>1</sup>D. E. Greiner *et al.*, Phys. Rev. Lett. **35**, 152 (1975).

<sup>2</sup>A. Goldhaber, Phys. Lett. **53B**, 306 (1974).

<sup>3</sup>T. Fujita and J. Hüfner, Nucl. Phys. **A343**, 493 (1980).

<sup>4</sup>I. Tanihata, Hyperfine Interact. **21**, 251 (1985).

<sup>5</sup>I. Tanihata *et al.*, Phys. Lett. **160B**, 380 (1985).

<sup>6</sup>E. J. Moniz *et al.*, Phys. Rev. Lett. **26**, 445 (1971).

<sup>7</sup>J. Hüfner and M. C. Nemes, Phys. Rev. C **23**, 2538 (1981).

<sup>8</sup>S. Shimoura *et al.*, Abstracts of Contributions to the Eleventh International Conference on Particles and Nuclei, Kyoto, 1987 (unpublished), p. 480.

<sup>9</sup>R. Serber, Phys. Rev. **72**, 1008 (1947).

<sup>10</sup>W. A. Friedman, Phys. Rev. C **27**, 569 (1983).

<sup>11</sup>I. Tanihata *et al.*, Phys. Rev. Lett. **55**, 2679 (1985).

<sup>12</sup>E. Arnold, Ph.D. thesis, University of Mainz, 1986 (unpublished).

<sup>13</sup>P. G. Hansen and B. Jonson, Europhys. Lett. **4**, 409 (1987).

<sup>14</sup>I. Tanihata, Nucl. Phys. **A478**, 795c (1988).

<sup>15</sup>B. G. Harvey, Nucl. Phys. **A444**, 498 (1985).

<sup>16</sup>B. G. Harvey, private communication.

<sup>17</sup>D. L. Olsen *et al.*, Phys. Rev. C **24**, 1529 (1981).

<sup>18</sup>I. Tanihata, private communication.